Multiscale modeling of martensitic phase transformations: On the numerical determination of heterogeneous mesostructures within shape-memory alloys induced by precipitates

T. Bartel, K. Hackl

The general scope of this contribution is the implementation of a micromechanical constitutive model for martensitic phase transformations based on energy-relaxation into the Multiscale Finite Element Method. Precisely, we study the effect of precipitates on the overall material response of a representative volume element (RVE), where the mesostructure of the material is fully resolved by the Finite Element discretization. The precipitate is modeled as an isotropic linear elastic and circular inclusion within a shape memory alloy (SMA) matrix, where in each Gauß-point of the matrix the aforementioned micromechanical model is applied. Providing macroscopic homogeneous deformations, we study the resulting phase distribution of austenite and martensite as well as the effective material response of the RVE. In particular, the energy minimizing displacement field turns out to be C^0-smooth and hence, the resulting phase distributions are heterogeneous.

1   Introduction

Recent developments in the field of materials science and materials engineering, respectively, require a sophisticated mechanical modeling of advanced materials like shape memory alloys (SMA). In this context, phenomenological models as for example proposed by Achenbach (1989); Huo and Müller (1993); Auricchio and Taylor (1997); Helm and Haupt (2003) are indispensable for efficient global algorithms and the simulation of large macroscopic problems. However, such models can not reproduce certain experimentally observed phenomena which have a significant impact on the overall material response.

In particular, Shaw and Kyriakides (1995); Ŝittner et al. (2005); Michutta and Somsen (2006), among others, point out that the phase distribution of austenite and martensite within Nickel-Titanium (NiTi) turns out to be heterogeneous. More precisely, Lüders-like deformation bands show up on all the material's scales which then propagate through the specimen. Hence, the volume fractions of the different phases are determined by the lath-width of these bands. In contrast to this, material models for SMAs generally yield 'smeared out' phase distributions revealing 'artificial' homogeneity.

This contribution aims at the analysis of the effect of precipitates on the overall material response of SMAs and the determination of such heterogeneous phase distributions, respectively. As for example highlighted by Tadaki et al. (1986); Bataillard et al. (1998); Khalil-Allafi et al. (2002); Michutta and Somsen (2006), Ni_4Ti_3 forms during the process of ageing, which enables the control of the Ni- and Ti-contents. These precipitates have a significant effect on the material behavior exemplified by phase evolutions, local stress fields and effective properties.

The model presented in this paper is constituted by the implementation of the micromechanically motivated constitutive law for martensitic phase transformations proposed by Bartel and Hackl (2009) (also outlined by Bartel and Hackl (2008)) into the Multiscale Finite Element Method. This micromechanical model is based on the concept of energy relaxation in combination with evolution equations derived from inelastic potentials. Energy relaxation methods are closely related to the direct methods in the calculus of variations (see e.g. Dacorogna (1982, 1989)). In this regard, these schemes aim at the determination of the so-called quasiconvex hull of an underlying energy functional, which is the optimum solution from the viewpoint of mathematics as for example elaborated by Morrey

(1952); Meyers (1965); Ball (1977); Ŝilhavy (1997). In this context, the model of Bartel and Hackl (2009) differs from relaxation-based concepts as for example proposed by Kohn and Strang (1983, 1986); Pagano et al. (1998); Ortiz and Repetto (1999); Govindjee and Miehe (2001); Govindjee et al. (2002); Stupkiewicz and Petryk (2002); Carstensen et al. (2002); Bartels et al. (2004); Hackl and Schmidt-Baldassari (2004); Govindjee et al. (2007); Hackl and Heinen (2008) in the sense that a distinct fluctuation field based on a mixture of first and second order laminates is defined taking into account an arbitrary number of martensite variants. All of the aforementioned models are designed to approximate the quasiconvex hull since an exact determination is only possible in rare cases as carried out by Kohn (1991); Smyshlyaev and Willis (1998) for a two- and three-well (geometrically linear) potential and by DeSimone and Dolzmann (1999, 2002) for nematic polymers even in the case of large deformations.

However, a full relaxation would contradict the hysteretic behavior clearly indicating that dissipative processes play a significant role. Therefore, the whole constitutive model is given by the relaxed free energy density and a dissipation functional in addition. The concept of dissipation functionals goes back to the works of Edelen (1973); Halphen and Nguyen (1975), for instance, and has been elaborated and enhanced by Hackl (1997); Ortiz and Stainier (1999); Mielke and Theil (1999); Mielke et al. (2002) among others. The application of a least-action principle to the enhanced total power of the system yields not only evolution equations but the yield criteria as well due to the specific choice of the dissipation potential.

The influence of precipitates on the material behavior is not modeled by means of simulating a precipitation process. These particles are rather supposed to maintain a steady-state and are thus modeled as fixed structure on the material's mesoscale. Precisely, these precipitates are discretized as circular inclusions within a solid SMA matrix where the geometry is fully resolved by Finite Elements. The transformation from the parent phase to such precipitates is taken into account by eigenstrains according to the change in the crystallographic lattice. The scale bridging from the macro- to the mesoscale is accomplished by the Multiscale Finite Element Method, where a fluctuation field is introduced as energy minimizer subjected to the fulfillment of the so-called Hill-Mandel microheterogeneity condition. The theory and application of the Multiscale Finite Element Method has been carried out for example by Feyel and Chaboche (2000); Miehe et al. (2002); Miehe and Dettmar (2004).

2 Micromechanical model

2.1 Transformation kinematics

Since martensitic transformations are diffusionless, the transition from one phase to another can be characterized by a (locally) homogeneous deformation of the crystal lattice according to Bain (1924) and related works by James and Hane (2000); Bhattacharya (2003), for example. This leads to the derivation of transformation or Bain-strains in terms of the right stretch tensor $\mathbf{U}^{tr}$. The restriction to small deformations enables the use of an additive decomposition of strains

$$\varepsilon_i = \varepsilon_i^{el} + \varepsilon_i^{tr} \tag{1}$$

for each phase i into elastic parts ε_i^{el} and inelastic parts $\varepsilon_i^{tr} = \mathbf{U}_i^{tr} - \mathbf{I}$ with $\mathbf{I}$ as the identity tensor. The number of phases to be taken into account depends upon the underlying material and the kind of transformation, respectively. Because of the reduction of crystallographic symmetry in going from austenite to martensite, there are NV (Number of Variants) variants of martensite possible. Precise values for ε_i^{tr} are provided in App. A which were taken from Bhattacharya (2003) and the references cited therein.

2.2 Constitutive model

In this subsection we elaborate on the derivation of a suitable hull for the energy density of the phase mixture. The first step in this regard is the definition of the mean energy density

$$\bar{\psi} = \left[1 - \sum_{i=1}^{NV} \theta_i \right] \psi_A \left(\varepsilon_A^{el} \right) + \sum_{i=1}^{NV} \theta_i \, \psi_i \left(\varepsilon_i^{el} \right) \tag{2}$$

with

$$\psi_A\left(\varepsilon_A^{el}\right) \quad := \quad \frac{1}{2}\,\varepsilon_A : \mathbf{E}_A : \varepsilon_A + c_A \tag{3}$$

$$\psi_i\left(\varepsilon_i^{el}\right) \quad := \quad \frac{1}{2}\left[\varepsilon_i - \varepsilon_i^{tr}\right] : \mathbf{E}_M : \left[\varepsilon_i - \varepsilon_i^{tr}\right] + c_M \tag{4}$$

as quadratic functionals for each phase. Here, ε_A and ε_I are averages of the strain-fields in each phase over representative volumes on the microscale. Later, however, we will describe them via explicit displacement fields introduced at the microscale. Furthermore, θ_i as introduced in (2) denotes the volume fraction of the $i-$th martensite variant subjected to the restrictions

$$r_i := -\theta_i \le 0 \ \forall i = 1, \ldots, NV \qquad \bar{r} := \sum_{i=1}^{NV} \theta_i - 1 \le 0 \quad , \tag{5}$$

$\mathbf{E}_\bullet$ is the elasticity tensor of austenite and martensite, respectively, and the quantities $c_\bullet$ are referred to as chemical energies for each phase, which can take temperature dependencies into account.

The open question is now, how the total strains within each phase, namely ε_A and $\varepsilon_i, i = 1, \ldots, NV$, can be determined by means of a suitable homogenization scheme. Within this work, we follow the concept of energy relaxation via lamination. This method aims at the approximation of the quasiconvex hull, which is defined as

$$Q\psi\left(\varepsilon\right) = \min\left\{\int_{[0,1]^d} \psi\left(\varepsilon + \nabla_S \varphi\right)\,dV\,;\varphi\right\} \tag{6}$$

in principle. In this context, $\varphi \in W_{\mathrm{per}}^{1,\infty}([0,1]^d, \mathbb{R}^d)$ symbolizes a fluctuation field superimposed onto the locally homogeneous deformations of a material point where $\nabla_S \bullet := \frac{1}{2}\left[\nabla \bullet + \bullet \nabla\right]$ and d denotes the spatial dimension of the underlying problem. The derivation of an exact quasiconvex hull, i.e. the finding of the optimum fluctuation φ among all admissible fields, is not possible in general. Therefore, φ is often specified in order to derive upper bounds to the quasiconvex hull (see for example Kohn and Strang (1983, 1986); Pagano et al. (1998); Govindjee and Miehe (2001); Govindjee et al. (2002); Stupkiewicz and Petryk (2002); Bartels et al. (2004); Govindjee et al. (2007) in this regard). The fluctuation field proposed by Bartel and Hackl (2009) is based on the spatial separation of the microscale - see Fig. 1 for a graphical illustration. Firstly, laminates of first order are introduced in order to distinguish between austenite and martensite in general. Furthermore, the martensite domain is subdivided into laminates of second order to take into account all crystallographic variants. Note that these laminates are aligned in different directions $\mathbf{n}_A$ and $\mathbf{n}_M$, respectively.
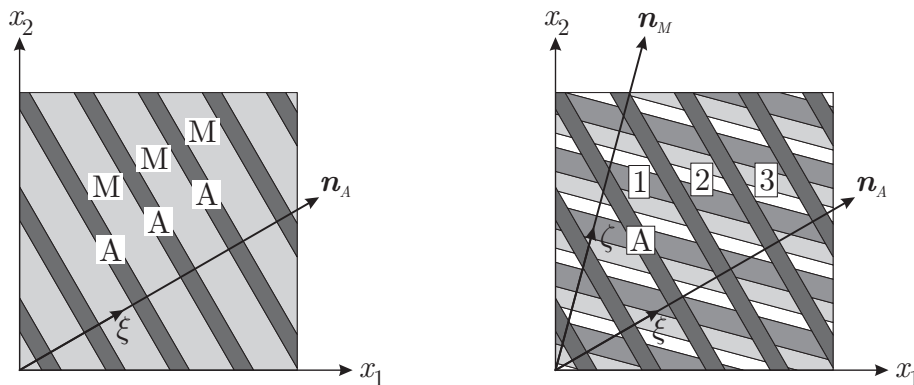
Figure 1 : According to Bartel and Hackl (2009), the microscale is spatially subdivided into first and second order laminates, which are aligned in different directions $\mathbf{n}_A$ and $\mathbf{n}_M$, respectively (here for the case of $NV = 3$).
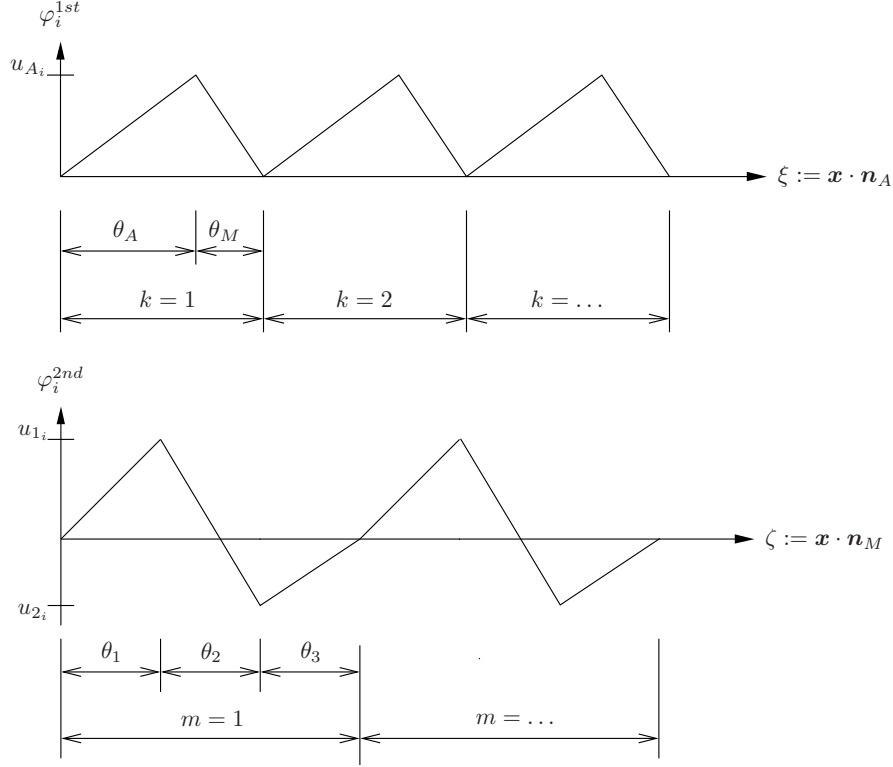
Figure 2 : According to the chosen microstructure, the locally homogeneous displacement field is enhanced by roof-like periodic fluctuations. They consist of a part φ^{1st} (top) and φ^{2nd} (bottom), the latter shown here for the exemplary case of $NV = 3$.

According to the chosen microstructure, the fluctuation field depicted in Fig. 2 is applied, which can mathematically be expressed by

$$
\varphi^{1st} := \begin{cases} \frac{1}{\theta_A} \mathbf{u}_A \left[\xi - k + 1\right] & \text{,if } k - 1 \leq \xi \leq k - 1 + \theta_A \\ -\frac{1}{\theta_M} \mathbf{u}_A \left[\xi - k\right] & \text{, else} \end{cases} \tag{7}
$$

and in case of $k - 1 + \theta_A < \xi \leq k$

$$
\varphi^{2nd}_I := -\frac{1}{\theta_I} \left[\mathbf{u}_I - \mathbf{u}_{I-1}\right] \left[\zeta - \sum_{n=1}^{I-1} \theta_n - (m-1) \theta_M\right] + \mathbf{u}_{I-1} \quad , I = 1, \dots, NV \tag{8}
$$

with $\mathbf{u}_0 = \mathbf{u}_{NV} = \mathbf{0}$. Thus, the total displacement field on the microscale

$$
\mathbf{u}(\mathbf{x}) = \varepsilon \cdot \mathbf{x} + \varphi(\mathbf{x}) \tag{9}
$$

with

$$
\varphi(\mathbf{x}) := \varphi^{1st} + \begin{cases} 0 & \text{,if } k - 1 \leq \xi \leq k - 1 + \theta_A \\ \varphi^{2nd}_1 & \text{,if } k - 1 + \theta_A < \xi \leq k \wedge m - 1 \leq \zeta \leq m - 1 + \theta_1 \\ \varphi^{2nd}_2 & \text{,if } k - 1 + \theta_A < \xi \leq k \wedge m - 1 + \theta_1 \leq \zeta \leq m - 1 + \theta_1 + \theta_2 \\ \dots \\ \varphi^{2nd}_{NV} & \text{,if } k - 1 + \theta_A < \xi \leq k \wedge m - 1 + \sum_{n=1}^{NV-1} \theta_n \leq \zeta \leq m - 1 + \sum_{n=1}^{NV} \theta_n \end{cases} \tag{10}
$$

depends on the mesoscopic strains ε as well as the so-called amplitudes of the fluctuation fields $\mathbf{u}_\bullet$, the projections $\xi := \mathbf{x} \cdot \mathbf{n}_A$, $\zeta := \mathbf{x} \cdot \mathbf{n}_M$, the mean phase fractions $\theta_M := \sum_{i=1}^{NV} \theta_i$, $\theta_A = 1 - \theta_M$ and multiples of an arbitrary

microscopic unit length k and m, respectively. With the enhanced displacement field at hand, the strains $\tilde{\varepsilon}(\mathbf{x})$ on the microscale can be obtained in a straight forward way via $\tilde{\varepsilon}(\mathbf{x}) = \varepsilon + \nabla_S \varphi$ which yields

$$\varepsilon_A \;=\; \varepsilon + \frac{1}{\theta_A}\, \mathbf{n}_A \otimes_S \mathbf{u}_A \tag{11}$$

$$\varepsilon_I \;=\; \varepsilon - \frac{1}{\theta_M}\, \mathbf{n}_A \otimes_S \mathbf{u}_A + \frac{1}{\theta_I}\, \mathbf{n}_M \otimes_S [\mathbf{u}_I - \mathbf{u}_{I-1}] \quad , I = 1,\dots,NV \tag{12}$$

These strains, which are constant in each phase, display compatibility properties in terms of rank-one connections for example according to Ball and James (1987) – here in a symmetrized form in the geometrically linear case. Moreover, the mean value of microscopic strains is equal to the macroscopic ones according to

$$\theta_A\, \varepsilon_A + \sum_{I=1}^{NV} \theta_i\, \varepsilon_I = \varepsilon \quad . \tag{13}$$

As can be estimated from (3), (4), stresses turn out not to be homogeneous on the microscale.

In contrast to the quantities $\mathbf{n}_\bullet$ and in particular θ_i, the evolution of the amplitudes $\mathbf{u}_\bullet$ is assumed to be purely energetic in nature. Hence, they are determined via the stationarity conditions

$$\frac{\partial \bar{\psi}}{\partial \mathbf{u}_A} = \mathbf{0} \quad , \frac{\partial \bar{\psi}}{\partial \mathbf{u}_I} = \mathbf{0} \quad , I = 1,\dots,NV-1 \qquad . \tag{14}$$

Solution of these yield

$$\mathbf{u}_A^* \;=\; -\widehat{\mathbf{E}}^{-1} \cdot \left[\Delta \mathbf{E} : \varepsilon + \frac{1}{\theta_M} \bar{\tau}^{tr} \right] \cdot \mathbf{n}_A \quad , \tag{15}$$

$$\mathbf{u}_I^* \;=\; -\frac{1}{\theta_M} \widehat{\mathbf{E}}_M^{-1} \cdot \left[\sum_{i=1}^{I} \sum_{j=I+1}^{NV} \theta_i \theta_j \left[\tau_j^{tr} - \tau_i^{tr} \right] \right] \cdot \mathbf{n}_M \tag{16}$$

as optimum values with $\Delta \mathbf{E} := \mathbf{E}_A - \mathbf{E}_M$, $\widehat{\mathbf{E}} := \mathbf{n}_A \cdot \tilde{\mathbf{E}} \cdot \mathbf{n}_A$, $\tilde{\mathbf{E}} := \frac{1}{\theta_A} \mathbf{E}_A + \frac{1}{\theta_M} \mathbf{E}_M$, $\widehat{\mathbf{E}}_M := \mathbf{n}_M \cdot \mathbf{E}_M \cdot \mathbf{n}_M$, $\tau_i^{tr} := \mathbf{E}_M : \varepsilon_i^{tr}$, $\bar{\tau}^{tr} := \sum_{i=1}^{NV} \theta_i \tau_i^{tr}$. With these derivations as well as (11), (12) and (2) at hand, a partially relaxed energy density

$$\psi_{rel}(\varepsilon, \mathbf{p}) \;=\; \frac{1}{2} \varepsilon : \bar{\mathbf{E}} : \varepsilon + \varepsilon : [[\Delta \mathbf{E} \cdot \mathbf{n}_A] \cdot \mathbf{u}_A^*] + \frac{1}{2} \mathbf{u}_A^* \cdot \widehat{\mathbf{E}} \cdot \mathbf{u}_A^* - \bar{\tau}^{tr} : \varepsilon$$
$$+ \frac{1}{\theta_M} \left[\bar{\tau}^{tr} \cdot \mathbf{n}_A \right] \cdot \mathbf{u}_A^* - \frac{1}{2} \sum_{I=1}^{NV} \left[\tau_I^{tr} \cdot \left[\mathbf{u}_I^* - \mathbf{u}_{I-1}^* \right] \right] \cdot \mathbf{n}_M + \bar{c} \tag{17}$$

with $\bar{\mathbf{E}} := \theta_A\, \mathbf{E}_A + \theta_M\, \mathbf{E}_M$ and $\bar{c} := \theta_A\, c_A + \theta_M\, c_M + \frac{1}{2} \sum_{I=1}^{NV} \theta_I\, \tau_I^{tr} : \varepsilon_I^t$ is obtained. Here,

$$\mathbf{p} = \{\theta_1,\dots,\theta_{NV}, \mathbf{n}_A, \mathbf{n}_M\} \tag{18}$$

denotes the list of all variables which are not assumed to minimize the energy density of the phase mixture but which are rather associated with dissipative processes leading to the well-known hysteretic material response of SMAs. The treatment of $\mathbf{p}$ will be elaborated in the subsequent section. The effective material response in terms of elastic stresses can be deduced from (17) via

$$\boldsymbol{\sigma} := \frac{\partial \psi_{rel}}{\partial \varepsilon} = \bar{\mathbf{E}} : \varepsilon + [\Delta \mathbf{E} \cdot \mathbf{n}_A] \cdot \mathbf{u}_A^* - \bar{\tau}^{tr} \quad . \tag{19}$$

2.3 Evolution equations

Following Halphen and Nguyen (1975), thermodynamical fluxes

$$\mathbf{q} = -\frac{\partial \psi_{rel}}{\partial \mathbf{p}} \tag{20}$$

can be determined, which are often referred to as thermodynamical conjugated forces or driving forces. Here, these fluxes are given by

$$
\begin{aligned}
q_I &= \frac{1}{2}\boldsymbol{\varepsilon} : \Delta\mathbf{E} : \boldsymbol{\varepsilon} + \boldsymbol{\tau}_I^{tr} : \left[\boldsymbol{\varepsilon} - \frac{1}{2}\boldsymbol{\varepsilon}_I^{tr}\right] + \frac{1}{2\,\theta_I^2}\left[\mathbf{u}_I - \mathbf{u}_{I-1}\right] \cdot \widehat{\mathbf{E}}_M \cdot \left[\mathbf{u}_I - \mathbf{u}_{I-1}\right] \\
&\quad -\frac{1}{2}\mathbf{u}_A \cdot \left[\mathbf{n}_A \cdot \left[\frac{1}{\theta_A^2}\mathbf{E}_A - \frac{1}{\theta_M^2}\mathbf{E}_M\right] \cdot \mathbf{n}_A\right] \cdot \mathbf{u}_A + \mathbf{n}_A \cdot \left[\frac{1}{\theta_M^2}\bar{\boldsymbol{\tau}}^{tr} - \frac{1}{\theta_M}\boldsymbol{\tau}_I^{tr}\right] \cdot \mathbf{u}_A
\end{aligned}
\tag{21}
$$

for the volume fraction of martensite variant I as well as

$$
\begin{aligned}
\mathbf{q}_{\mathbf{n}_A} &= -\mathbf{u}_A \cdot \left[\tilde{\mathbf{E}} \cdot \mathbf{n}_A\right] \cdot \mathbf{u}_A - \boldsymbol{\varepsilon} : \Delta\bar{\mathbf{E}} \cdot \mathbf{u}_A - \frac{1}{\theta_M}\bar{\boldsymbol{\tau}}^{tr} \cdot \mathbf{u}_A \\
&\quad -\frac{1}{\theta_M}\sum_{i=1}^{NV-1}\mathbf{u}_A \cdot \left[\left[\mathbf{E}_{i+1} - \mathbf{E}_i\right] \cdot \mathbf{n}_M\right] \cdot \mathbf{u}_i
\end{aligned}
\tag{22}
$$

for the laminate normals $\mathbf{n}_A$ and $\mathbf{n}_M$, respectively. Apparently, these driving forces may cause the evolution of dissipative internal variables in the spirit of thermodynamics of irreversible processes. It goes back to Strutt (1873); Onsager (1931a,b) that the rates of internal variables have to obey certain principles related to dissipation. Here, we enhance the standard dissipation terms by a so-called dissipation potential $\Delta(\dot{\mathbf{p}})$, which has been introduced for the first time by Edelen (1973). According to Mielke and Theil (1999); Ortiz and Repetto (1999); Ortiz and Stainier (1999); Mielke et al. (2002), the application of a least-action principle to the sum of total power and the dissipation potential, namely $\mathcal{L} := \dot{\psi}_{rel} + \Delta(\dot{\mathbf{p}})$, results in the differential inclusion

$$-\mathbf{q} + \frac{\partial \Delta(\dot{\mathbf{p}})}{\partial \dot{\mathbf{p}}} \in \mathbf{0} \tag{24}$$

giving the rates of internal variables $\dot{\mathbf{p}}$ as minimizers of $\mathcal{L}$ in an implicit form. For convenience with respect to the algorithmical implementation, a dual dissipation functional

$$\Delta^* := \max\left\{\mathbf{q} \cdot \dot{\mathbf{p}} - \Delta(\dot{\mathbf{p}})\,;\dot{\mathbf{p}}\right\} \tag{25}$$

can be defined via the Legendre-Fenchel transform, which then yields

$$\dot{\mathbf{p}} \in \frac{\partial \Delta^*(\mathbf{p})}{\partial \mathbf{p}} \tag{26}$$

as evolution euqations for $\mathbf{p}$. Furthermore, the introduction of Δ and the aforementioned scheme allow us to derive characteristic functions Φ (or yield functions) instead of supposing them due to empirical knowledge. As for example shown by Bartel and Hackl (2009), any contribution to Δ being homogeneous of first order will result

in the so-called indicator function

$$\Delta^* = \begin{cases} 0 & \text{, if } \Phi \leq 0 \\ \infty & \text{, else} \end{cases} \tag{27}$$

in terms of the dual dissipation functional. Thus, such terms within Δ will define the characteristic function Φ, which separates elastic from inelastic material behavior. Furthermore, any contribution in Δ which is not homogeneous of first order will cause the evolution law to become rate dependent, or in other terms, the material behavior becomes viscous.

Here, we use

$$\Delta := k_\theta \sum_{i=1}^{NV} |\dot{\theta}_i| + k_n \left[\|\dot{\boldsymbol{n}}_A\| + \|\dot{\boldsymbol{n}}_M\| \right] \tag{28}$$

which results in a classical rate-independent plasticity type evolution law

$$\dot{\theta}_I = \lambda_I^\theta \, \text{sign} \, (q_I) \, , I = 1, \dots, NV \tag{29}$$

$$\dot{\mathbf{n}}_A = \lambda_{\mathbf{n}_A} \frac{\mathbf{q}_{\mathbf{n}_A}}{\|\mathbf{q}_{\mathbf{n}_A}\|} \tag{30}$$

$$\dot{\mathbf{n}}_M = \lambda_{\mathbf{n}_M} \frac{\mathbf{q}_{\mathbf{n}_M}}{\|\mathbf{q}_{\mathbf{n}_M}\|} \tag{31}$$

with characteristic functions

$$\Phi_I = |q_I| - k_\theta \, , I = 1, \dots, NV \tag{32}$$

$$\Phi_{\mathbf{n}_A} = \|\mathbf{q}_{\mathbf{n}_A}\| - k_n \tag{33}$$

$$\Phi_{\mathbf{n}_M} = \|\mathbf{q}_{\mathbf{n}_M}\| - k_n \tag{34}$$

and complementary conditions

$$\Phi_\bullet \leq 0, \quad \lambda_\bullet \geq 0, \quad \Phi_\bullet \lambda_\bullet = 0 \tag{35}$$

where $\lambda_\bullet$ denotes consistency parameters. For simplicity, we assume now that the laminate directions will remain constant after the phase transformations have been initiated. The consideration of changing laminate orientations can yield interesting results, though, as for example shown by Bartel (2009).

Such restrictions as exemplified by (35) are treated via predictor corrector schemes by default. Here, a more sophisticated way is adopted which is also elaborated in Bartel and Hackl (2009) making use of the so-called Fischer-Burmeister complementary functions. This ansatz results in the substitution of (35) by

$$\sqrt{\Phi_\bullet^2 + \lambda_\bullet^2} + \Phi_\bullet - \lambda_\bullet = 0 \quad . \tag{36}$$

In the same manner, the conservation of mass reflected by (5) can be accounted for by means of

$$\sqrt{r_I^2 + \Lambda_I^2} + r_I - \Lambda_I = 0 \quad , I = 1, \dots, NV \tag{37}$$

$$\sqrt{\bar{r}^2 + \Gamma^2} + \bar{r} - \Gamma = 0 \quad . \tag{38}$$

The additional consistency parameters Λ_I and Γ enter the model via enhanced driving forces

$$q_I^{enh} := q_I + \Lambda_I - \Gamma \quad , I = 1, \dots, NV \tag{39}$$

replacing (21).

3 Mesoscopic model

3.1 Problem discretization

As for example pointed out by Tadaki et al. (1986); Tirry and Schryvers (2005); Michutta and Somsen (2006), Ni_4Ti_3 precipitates occur as disc-like particles within NiTi shape memory alloys during the process of ageing (see Fig. 3). This technique is suitable for the precise control of the Ni-content within the alloy which highly affects the martensite start temperature, for instance (see Khalil-Allafi et al. (2002) among others). After a stress free ageing process, these lenticular precipitates (diameter $70 - 900\,\mathrm{nm}$, depth $6 - 70\,\mathrm{nm}$, volume fraction $2.5 - 9.0\,\%$) are uniformly distributed along crystallographic $\langle 111 \rangle$ planes. In case of Ni_4Ti_3, the rhombohedric structure can be deduced from 27 body centered cubic unit cells of austenite subject to the substitution of the central Ti- by a Ni-atom. However, Tadaki et al. (1986) point out that the crystal structure does not completely coincide with this theory and that the lattice within the precipitate is compressed. This leads to the occurrence of eigenstrain and eigenstress fields, respectively, which are also experimentally validated for example by Tirry and Schryvers (2005).

Here, the precipitate is modeled as centric circular inclusion within a SMA matrix (see Fig. 4). The size of the square RVE is one unitlength where the center of the underlying cartesian coordinate system lies in the center of the square. Whereas the micromechanical model presented in the previous sections is applied in each Gauß-point of the matrix, the material behavior of the precipitate is assumed to be isotropic linear elastic. In particular, the material parameters are given by

$$\text{Young's modulus austenite} \quad : \quad E_A = 83\,\mathrm{GPa} \tag{40}$$

$$\text{Young's modulus martensite} \quad : \quad E_M = 34\,\mathrm{GPa} \tag{41}$$

$$\text{Poisson's ratio austenite/martensite} \quad : \quad \nu_A = \nu_M = 0.33 \tag{42}$$

$$\text{Difference in chemical energies} \quad : \quad c_M - c_A = 0.024\,\mathrm{GPa} \tag{43}$$

for the matrix material as well as

$$\text{Young's modulus inclusion} \quad : \quad E_{inc} = 34\,\mathrm{GPa} \tag{44}$$

$$\text{Poisson's ratio inclusion} \quad : \quad \nu_{inc} = 0.33 \tag{45}$$

for the inclusion. The dissipation coefficient is chosen as $k_\theta = 0.01$ GPa/s. According to Tirry and Schryvers
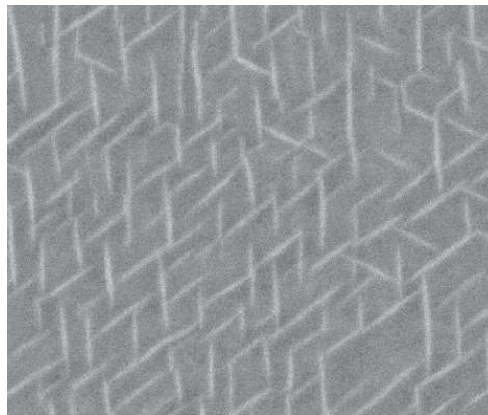
Figure 3 : Precipitates within NiTi shape memory alloys occur due to the process of ageing and form as disc-like particles which are, in the absence of applied stresses, uniformly distributed along crystallographic $\langle 111 \rangle$ planes (courtesy of C. Somsen).
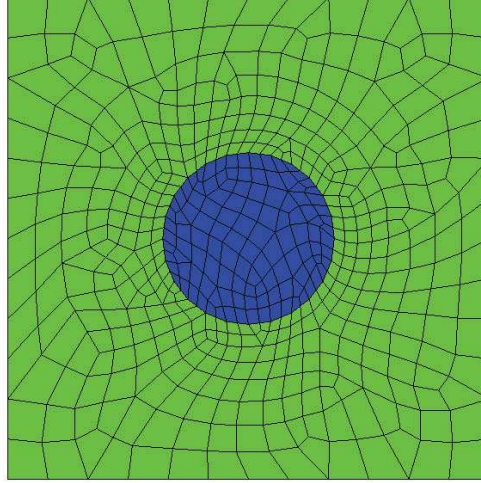
Figure 4 : The RVE is chosen as square with a unit width of 1. Inside the SMA matrix (green) lies the circular precipitate (blue) which is supposed to be isotropic linear elastic.

(2005), the eigenstrain of the precipitate is given by

$$\varepsilon_P = -0.005 \, \mathbf{e}_1 \otimes \mathbf{e}_1 - 0.005 \, \mathbf{e}_2 \otimes \mathbf{e}_2 \quad , \tag{46}$$

which results in $\varepsilon_P^{el} = \varepsilon - \varepsilon_P$ as elastic strains within the inclusion.

The effective material behavior on the level of the mesoscopic RVE is determined via the so-called multiscale Finite Element Method (abbreviated by MFEM from now on). Among other homogenization schemes as for example proposed by Voigt (1889); Reuss (1929); Hashin and Shtrikman (1962) this method represents the most flexible and comprehensive way to compute effective material properties. Moreover, it allows for the prediction of the spatial distribution and time evolution of internal variables. Even though (semi-)analytical homogenization schemes have been further developed (see e.g. Lielens (1999); Zheng and Du (2001); Pierard et al. (2004, 2007); Mercier and Molinari (2009)), the MFEM is the method of choice in particular in the context of inelastic material behavior.

A brief overview on the main aspects of the MFEM is given now. The vicinity of a macroscopic material point can be extended to a mesoscopic RVE where the underlying material sructure is fully resolved by the geometric discretization. The homogeneous part of the displacements on the mesoscale $\bar{\mathbf{u}}$ is hence given by $\mathbf{u}^{hom} = \varepsilon \cdot \mathbf{x}$, where ε denotes the macroscopic strain (for a specific material point) and $\mathbf{x}$ is the position on the mesoscale, here.

The influence of the mesoscopic inhomogeneities on the effective response of the RVE is taken into account via the introduction of a fluctuation field $\phi(\mathbf{x})$. This additional field is superimposed onto the locally homogeneous displacements by means of

$$\bar{\mathbf{u}}(\mathbf{x}) = \mathbf{u}^{hom} + \phi(\mathbf{x}) = \varepsilon \cdot \mathbf{x} + \phi(\mathbf{x}) \tag{47}$$

Thus, the strains within the RVE are given by

$$\bar{\varepsilon}(\mathbf{x}) = \varepsilon + \nabla_S \phi(\mathbf{x}) \quad . \tag{48}$$

Now, $\phi(\mathbf{x})$ is supposed to minimize the mesoscopic energy in terms of

$$\phi^*(\mathbf{x}) = \arg\min \left\{ \frac{1}{V} \int_\Omega \bar{\psi} \left(\varepsilon + \nabla_S \phi(\mathbf{x}) \right) \, \mathrm{d}V \right\} \quad . \tag{49}$$

Incidentally, this idea coincides with the concept of quasiconvexification as pointed out in one of the previous
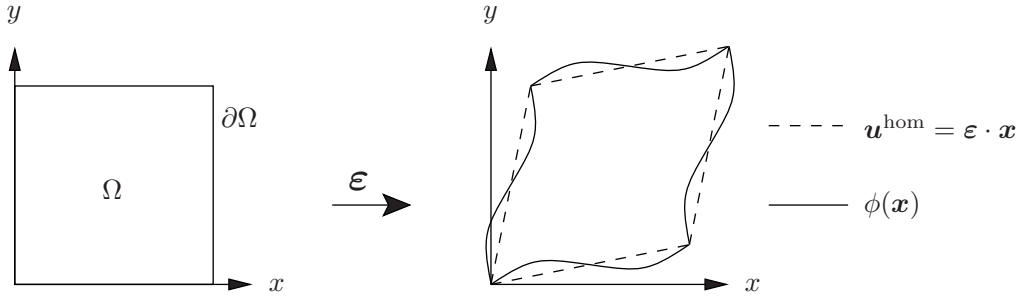
Figure 5 : The locally homogeneous displacements are enhanced by a fluctuation field $\phi(\mathbf{x})$ which is peri-
odic at the boundary $\partial\Omega$ in order to fulfill the Hill-Mandel microheterogeneity condition.

sections (see (6)).

Apparently, boundary conditions for $\phi(\mathbf{x})$ are not unique. Therefore, another criterion has to be established exemplified by the so-called Hill-Mandel microheterogeneity condition

$$\bar{\boldsymbol{\sigma}} : \dot{\bar{\boldsymbol{\varepsilon}}} = \frac{1}{V} \int_\Omega \boldsymbol{\sigma} : \dot{\boldsymbol{\varepsilon}} \, \mathrm{d}V \tag{50}$$

which is provided for the geometrically linear case, here. Among other choices, this condition is fulfilled by assuming that the fluctuation field $\phi(\mathbf{x})$ is periodic at the boundary $\partial\Omega$ of the RVE as illustrated in Fig. 5.

The effective material response of the RVE in terms of the elastic stresses is determined via

$$\bar{\boldsymbol{\sigma}} = \frac{1}{V} \int_\Omega \boldsymbol{\sigma}(\mathbf{x}) \, \mathrm{d}V \quad . \tag{51}$$

Mean values of any internal variable can be obtained in an analog manner.

3.2 Numerical examples

The mesoscopic RVE depicted in Fig. 4 is subjected to homogeneous deformations

$$\boldsymbol{\varepsilon} = \kappa(t) \, 0.055 \, \mathbf{e_1} \otimes \mathbf{e_1} \tag{52}$$

with $\kappa(t) = \sin(2\pi t)$, where $t \in [0, 1]$ is referred to as 'pseudo time' since the material behavior is rate independent. The volume fraction of the inclusion is chosen as 10% of the total volume of the RVE.

For a material undergoing a cubic to tetragonal transformation, the results in terms of a stress-strain diagram and the evolution of the averaged volume fraction of martensite variant 1, respectively, is depicted in Figs. 6 and 7. For several load steps, which are indicated in Fig. 6, the distribution of austenite and martensite variant 1 is illustrated in Figs. 8 and 9, which will be discussed in detail now.

As expected, the transformation from austenite to martensite is initiated at the upper and lower edge of the inclusion (step 10). The transformation proceeds in localized zones which suddenly stop to grow further in load step 13. From step 10 to 13, the stress-strain relation of the RVE is characterzied by a smoooth transition from a linear behavior to a pronounced stress plateau. Subsequently, martensite nuclei form within the matrix rather than at the boundary to the inclusion (steps 13 to 16). This martensite 'islands' grow towards each other forming 'mesoscopic laminates'. In fact, the mesoscale solely consists of pure phases. Furthermore, these laminates evolve perpendicular to their direction of alignment until the whole matrix has been transformed into martensite (steps
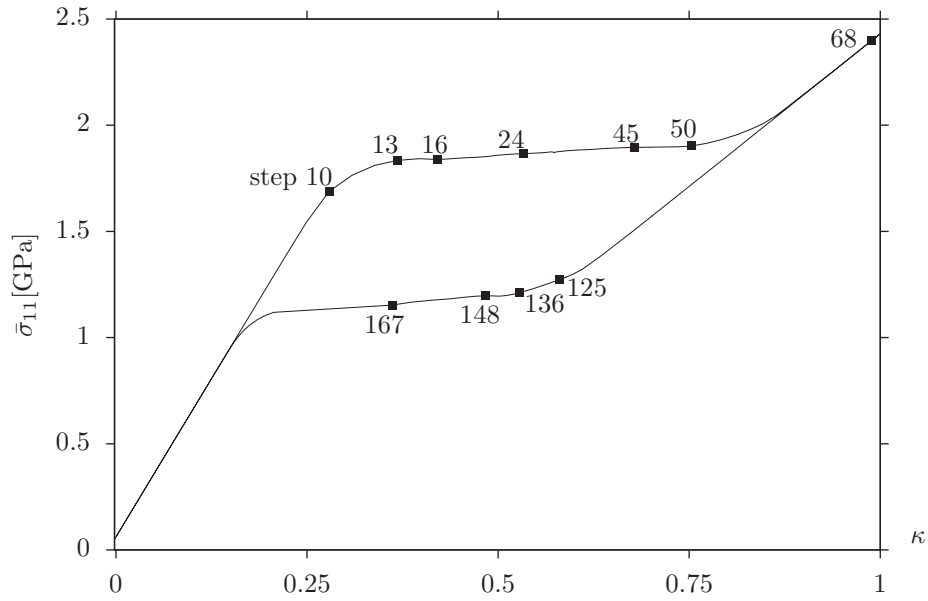
Figure 6 : The material response in terms of the mean stress component $\bar{\sigma}_{11}(\kappa)$ reveals the typical characteristics of SMAs mainly exemplified by the stress plateaus and hysteresis loop, respectively. The marked load steps indicate noteworthy points of the loading/unloading path (see Figs. 8,9).
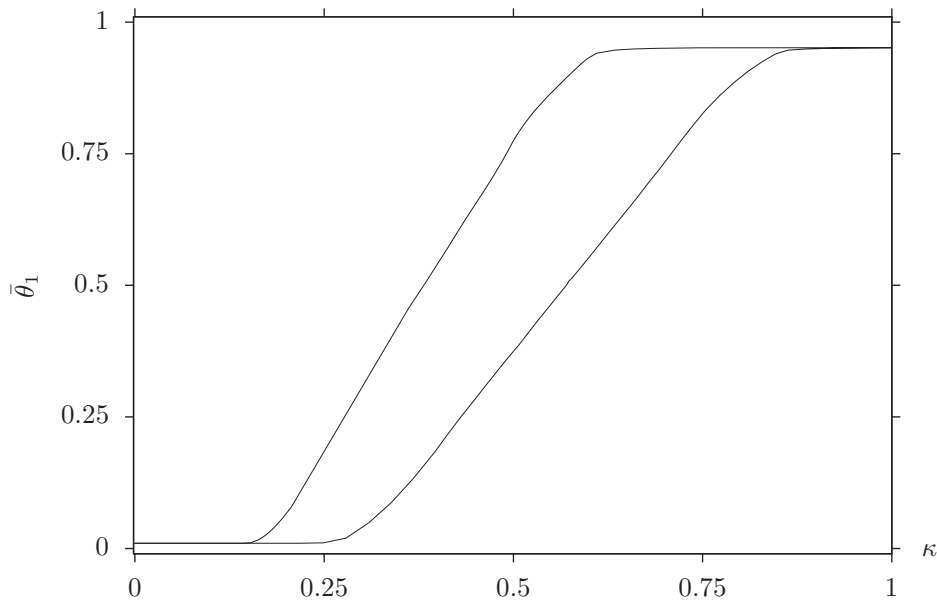
Figure 7 : Evolution of the mean volume fraction of martensite variant 1 depending upon the load factor κ.

45 to 68). During unloading, the transformation from martensite to austenite proceeds fairly similar to the loading case except for the fact that the laminates are oriented differently (steps 125 to 167).

We would like to particularly emphasize here, that the energetically favorable fluctuation field $\phi^*(\mathbf{x})$ according to (49) turns out to be C^0-smooth during the transformation. Fig. 11 shows the $x-$ and $y-$ component of the fluctuation field at the boundary $\partial\Omega$ of the RVE, where s denotes the coordinate along the boundary as indicated in Fig. 10 (left). Furthermore, Fig. 12 depicts both components of $\phi(\mathbf{x})$ along a certain line element defined in Fig. 10 (right), clearly indicating that the fluctuations are piecewise linear. On both material's scales considered here, roof-like displacement fields play a key role - as part of the constitutive model (micromechanical model) and as solution of a global computation scheme (MFEM).

4 Conclusions

The application of fluctuation fields constitutes a suitable scheme independent of the observed material scale in order to determine a mathematically and physically reasonable energy density and thus, a sound constitutive law. It is mathematically reasonable since the introduction of fluctuations are employed to approximate the so-called quasiconvex envelope, which guarantees the existence of a solution and moreover mesh-independent results in the context of the FEM. Furthermore, it is physically reasonable because the solution of the mesoscopic problem is characterized by heterogeneous phase distributions which are also experimentally observed. In particular, the mesocopic RVE only consists of pure phases (100% austenite or 100% martensite) and the overall amount of martensite, for instance, is determined by the lath-width of the mesoscopic laminates which occur during the loading-unloading process. In this sense, the presented multiscale model predicts the influence of precipitates on the material behavior accurately.

Among other meaningful extensions of the model, like the consideration of anisotropic elastic properties of each phase or the thermomechanical coupling, the consideration of another martensitic phase, namely the so-called R-phase, is a promising future objective. As indicated in experiments for example by Michutta and Somsen (2006), the computations could particularly improve the understanding concerning the fact, that the eigenstains corresponding to the formation of precipitates favor the evolution of the so-called R-phase.

A Bain strains

According to Bhattacharya (2003), Bain-strains can be derived for the geometrically linear case as

$$\varepsilon_1^{tr} = \begin{pmatrix} \alpha & 0 & 0 \\ 0 & \beta & 0 \\ 0 & 0 & \beta \end{pmatrix} \tag{53}$$

$$\varepsilon_2^{tr} = \begin{pmatrix} \beta & 0 & 0 \\ 0 & \alpha & 0 \\ 0 & 0 & \beta \end{pmatrix} \tag{54}$$

$$\varepsilon_3^{tr} = \begin{pmatrix} \beta & 0 & 0 \\ 0 & \beta & 0 \\ 0 & 0 & \alpha \end{pmatrix} \tag{55}$$

for cubic to tetragonal martensitic transformations with $\alpha = 0.0221$, $\beta = -0.111$.
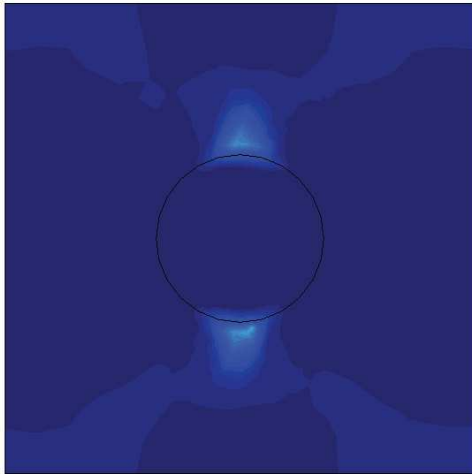
step 10
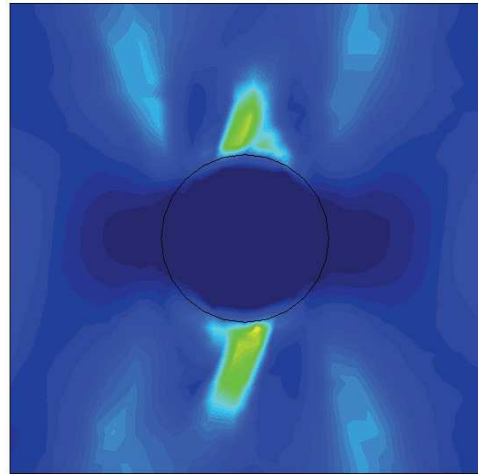
step 13
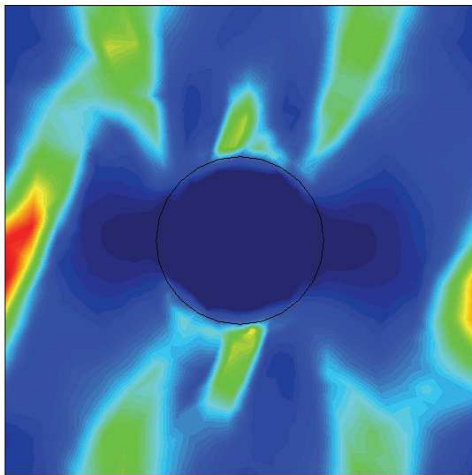
step 16
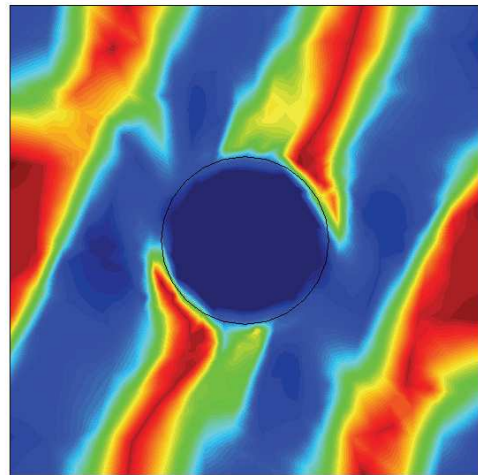
step 24
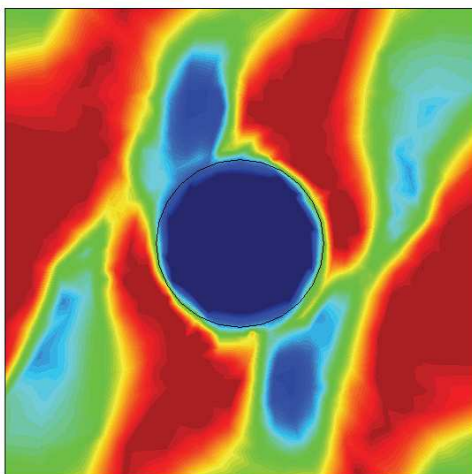
step 45
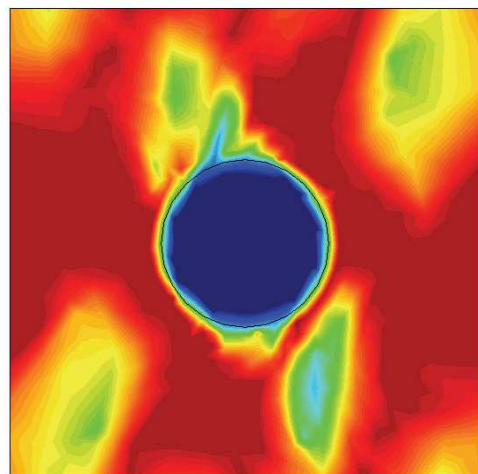
step 50

Figure 8 : Spatial distribution of austenite and martensite variant 1 at different load steps during loading. Most significantly, the phases arrange themselves in 'pure' domains of austenite and martensite, respectively, resulting in heterogeneous mesostructures.
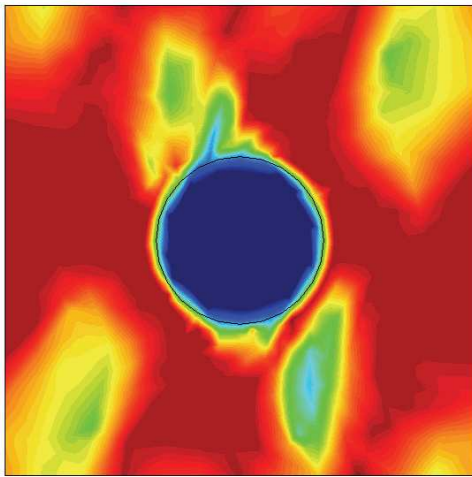
step 50
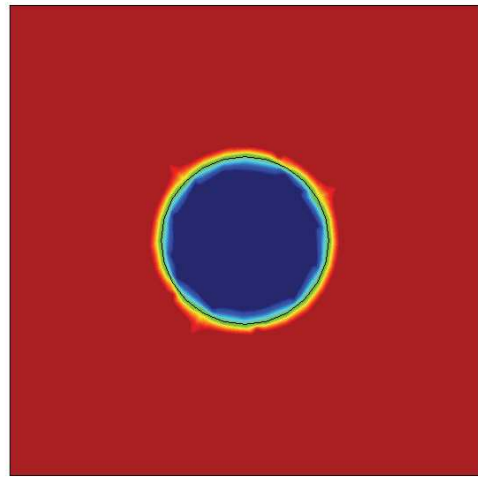
step 68
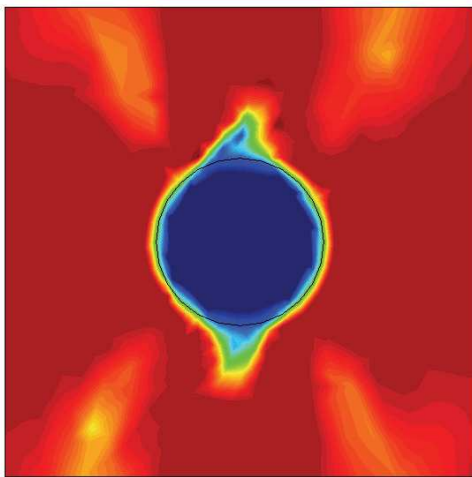
step 125
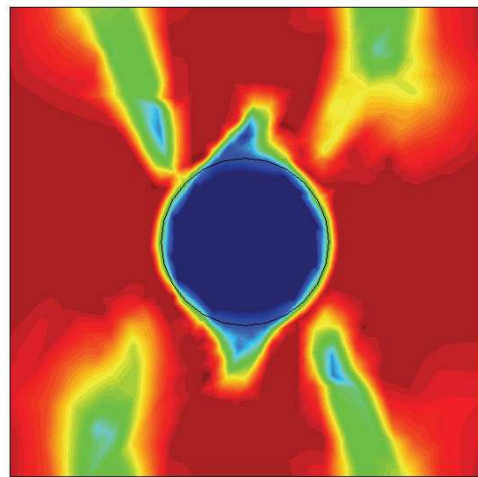
step 136
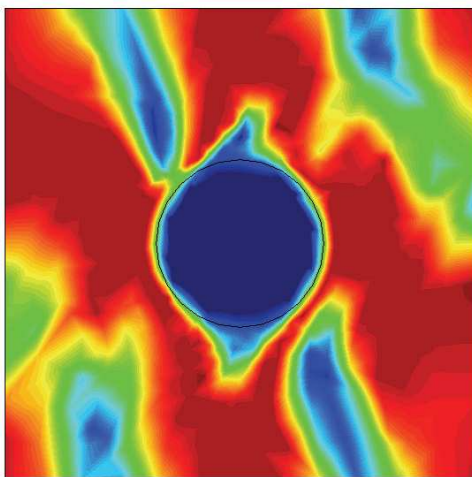
step 148
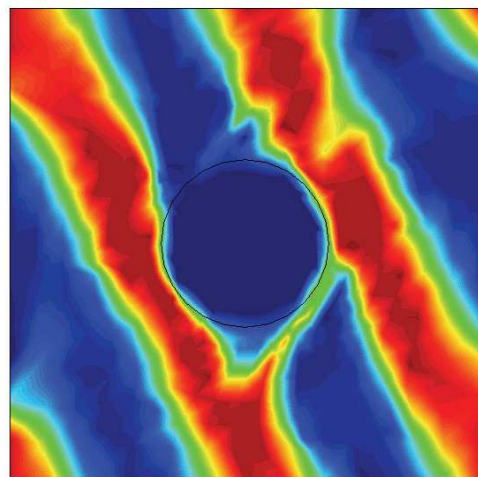
step 167

Figure 9 : Spatial distribution of austenite and martensite variant 1 at different load steps during unloading.
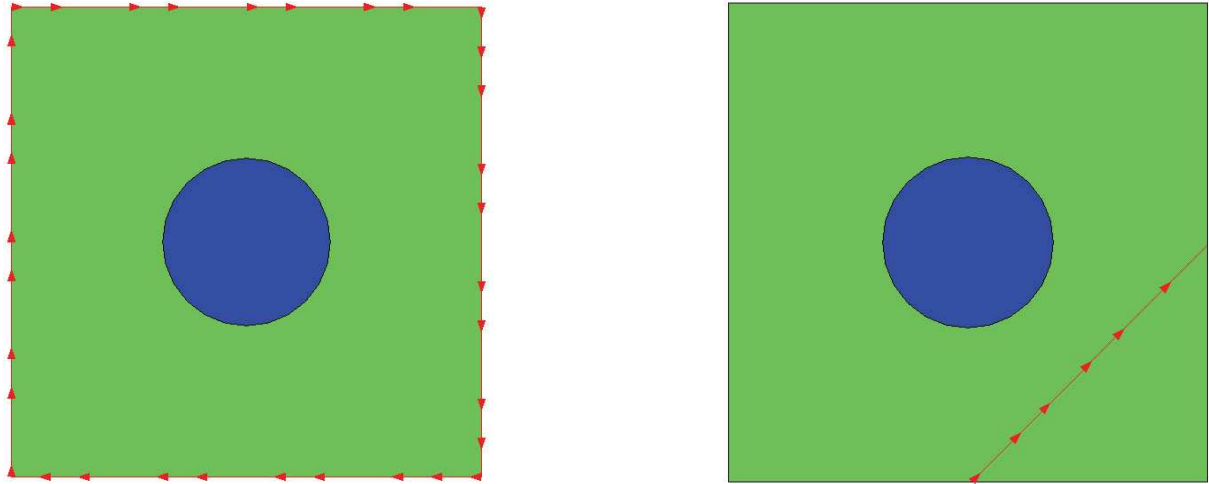
Figure 10 : Definition of a local coordinate s along the boundary $\partial\Omega$ of the RVE (left,see results depicted in Fig. 11) and through the RVE (right,see results depicted in Fig. 12), respectively.
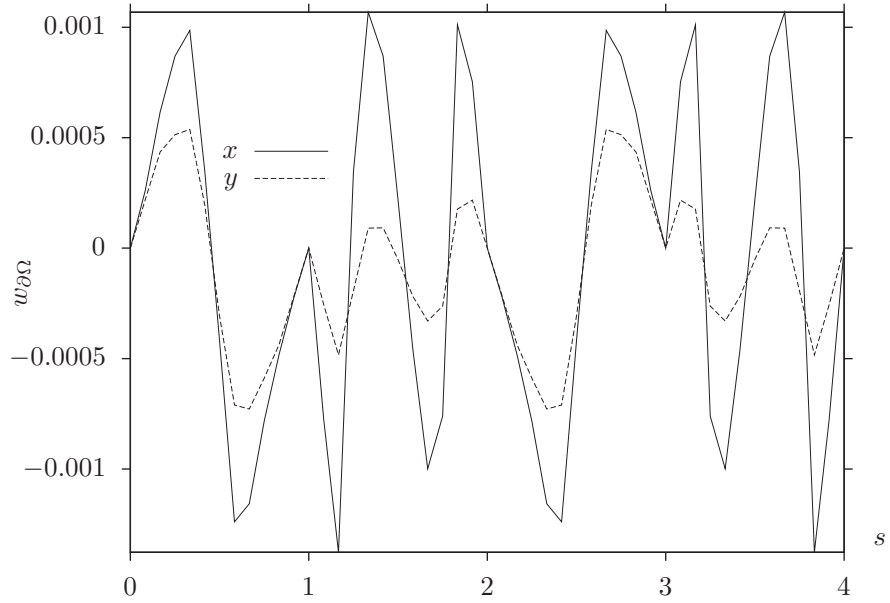
Figure 11 : Fluctuations $\phi(\partial\Omega)$ at the boundary of the RVE.
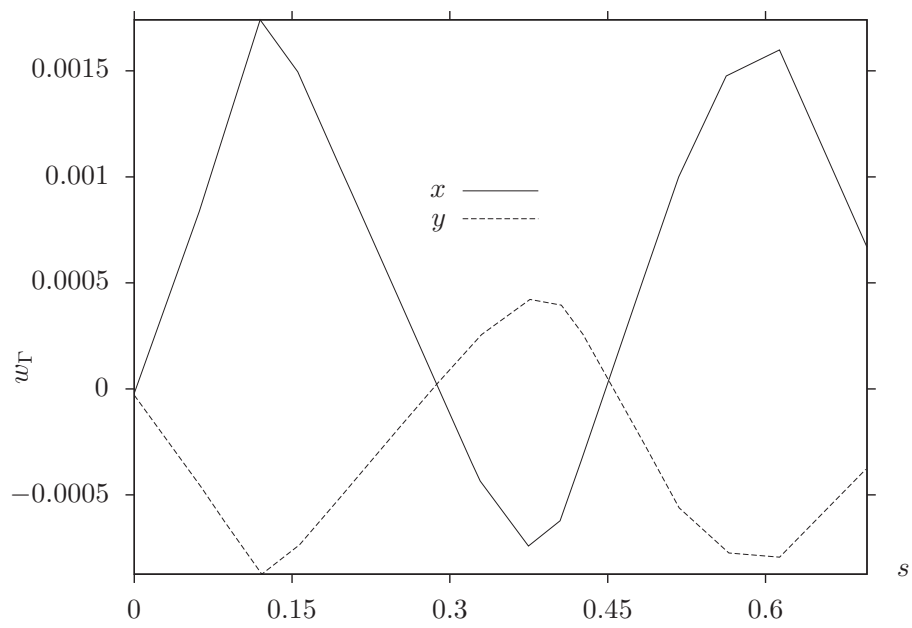
Figure 12 : Fluctuations $\phi(s)$ along a local coordinate s through the RVE. In fact, the energetically favorable fluctuation field is characterized by C^0-smooth piecewise linear functions.

References

Achenbach, M.: A model for an alloy with shape memory. *Int. J. Plast.*, 5, (1989), 371–395.

Auricchio, F.; Taylor, R.: Shape-memory alloys: modelling and numerical simulations of the finite-strain superelastic behavior. *Comp. Meth. Appl. Mech. Engrg.*, 143, (1997), 175–194.

Bain, E. C.: The nature of martensite. *Trans. AIME*, 70, (1924), 25.

Ball, J.: Convexitiy conditions and existence theorems in nonlinear elasticity. *Arch. Rat. Mech. Anal.*, 63, (1977), 337–403.

Ball, J.; James, R.: Fine phase mixtures as minimizers of energy. *Arch. Rat. Mech. Anal.*, 100, (1987), 13–52.

Bartel, T.: Dissertation, Ruhr-Universität Bochum, http://www.iofm.de/en/institute/team/senior_researchers/ (2009), Mitteilungen aus dem Institut fuer Mechanik Nr. 150.

Bartel, T.; Hackl, K.: A novel approach to the modelling of single-crystalline materials undergoing martensitic phase-transformations. *Mat. Sci. Engrg. A*, 481–482, (2008), 371–375.

Bartel, T.; Hackl, K.: A micromechanical model for martensitic phase-transformations in shape-memory alloys based on energy-relaxation. *Z. Angew. Math. Mech.*, 89 (10), (2009), 792–809, DOI: 10.1002/zamm.200900244.

Bartels, S.; Carstensen, C.; Hackl, K.; Hoppe, U.: Effective relaxation for microstructure simulations: algorithms and applications. *Comp. Methods Appl. Mech. Engrg.*, 193, (2004), 5143–5175.

Bataillard, L.; Bidaux, J.-E.; Gotthardt, R.: Interaction between microstructure and multiple–step transformation in binary NiTi alloys using *in–situ* transmission electron microscopy observations. *Phil. Mag. A*, 78, (1998), 327–344.

Bhattacharya, K.: *Microstructure of Martensite - Why it forms and how it gives rise to the shape-memory effect*. Oxford University Press, New York (2003).

Carstensen, C.; Hackl, K.; Mielke, A.: Nonconvex potentials and microstructures in finite-strain plasticity. *Proc. Roy. Soc. London A*, 458, (2002), 299–317.

Dacorogna, B.: Quasiconvexity and relaxation of the nonconvex problems in the calculus of variations. *J. Func. Anal.*, 46, (1982), 102–118.

Dacorogna, B.: *Direct Methods in the Calculus of Variations*. Springer, Berlin (1989).

DeSimone, A.; Dolzmann, G.: Material instabilities in nematic polymers. *Physica D*, 136, (1999), 175–191.

DeSimone, A.; Dolzmann, G.: Macroscopic response of nematic elastomers via relaxation of a class of SO(3)-invariant energies. *Arch. Rat. Mech. Anal.*, 161, (2002), 181–204.

Edelen, D. G. B.: On the existence of symmetry relations and dissipation potentials. *Arch. Rat. Mech. Anal.*, 51, (1973), 218–227.

Feyel, F.; Chaboche, J. L.: FE^2 multiscale approach for modelling the elastoviscoplastic behaviour of long fibre sic/ti composite materials. *Comp. Meth. Appl. Mech. Engrg.*, 183, (2000), 215–232.

Govindjee, S.; Hackl, K.; Heinen, R.: An upper bound to the free energy of mixing by twin-compatible lamination for n-variant martensitic phase transformations. *Continuum Mech. Thermodyn.*, 18, (2007), 443–453.

Govindjee, S.; Miehe, C.: A multi-variant martensitic phase transformation model: formulation and numerical implementation. *Comp. Methods Appl. Mech. Engrg.*, 191, (2001), 215–238.

Govindjee, S.; Mielke, A.; Hall, G.: The free energy of mixing for n-variant martensitic phase transformations using quasi-convex analysis. *J. Mech. Phys. Sol.*, 50, (2002), 1897–1922.

Hackl, K.: Generalized standard media and variational principles in classical and finite strain elastoplasticity. *J. Mech. Phys. Sol.*, 45, (1997), 667–688.

Hackl, K.; Heinen, R.: A micromechanical model for pretextured polycrystalline shape–memory alloys including elastic anisotropy. *Continuum Mech. Thermodyn.*, 19, (2008), 499–510.

Hackl, K.; Schmidt-Baldassari, M.: A micromechanical model for polycrystalline shape-memory alloys. *Mat. Sc. Eng. A*, 378, (2004), 503–506.

Halphen, B.; Nguyen, Q. S.: Sur les matériaux standards généralisés. *J. Mécanique*, 14, (1975), 39–63.

Hashin, Z.; Shtrikman, S.: A variational approach to the theory of the elastic behaviour of multiphase materials. *J. Mech. Phys. Sol.*, 11, (1962), 127–140.

Helm, D.; Haupt, P.: Shape memory behaviour: modelling within continuum mechanics. *Int. J. Sol. Struct.*, 40, (2003), 827–849.

Huo, Y.; Müller, I.: Nonequilibrium thermodynamics of pseudoelasticity. *Cont. Mech. Thermodyn.*, 5, (1993), 163–204.

James, R.; Hane, K.: Martensitic transformations and shape memory materials. *Acta mater.*, 48, (2000), 197–222.

Khalil-Allafi, J.; Dlouhý, A.; Eggeler, G.: Ni_4Ti_3–precipitation during aging of NiTi shape memory alloys and its influence on martensitic phase transformations. *Acta Materialia*, 50, (2002), 4255–4274.

Kohn, R.: The relaxation of a double-well energy. *Cont. Mech. Thermodyn.*, 3, (1991), 193–236.

Kohn, R. V.; Strang, G.: Explicit relaxation of a variational problem in optimal design. *Bull. Am. Math. Soc.*, 9, (1983), 211–214.

Kohn, R. V.; Strang, G.: Optimal design and relaxation of variational problem i, ii, iii. *Comm. Pure Appl. Mech.*, 39, (1986), 113–137, 139–182, 353–377.

Lielens, G.: Micro-Macro modeling of structured materials (1999), PhD thesis.

Mercier, S.; Molinari, A.: Homogenization of elastic-viscoplastic heterogeneous materials: Self-consistent and Mori-Tanaka schemes. *International Journal of Plasticity*, 25, 6, (2009), 1024–1048.

Meyers, N. G.: Quasi–convexity and lower semicontinuity of multiple variational integrals of any order. *Trans. Amer. Math. Soc.*, 119, (1965), 225–249.

Michutta, J.; Somsen, C.: Elementary martensitic transformation processes in Ni–rich NiTi single crystals with Ni_4Ti_3 precipitates. *Acta Materialia*, 54, (2006), 3525–3542.

Miehe, C.; Dettmar, J.: A framework for micro–macro transitions in periodic particle aggregates of granular materials. *Comp. Meth. Appl. Mech. Engrg.*, 193, (2004), 225–256.

Miehe, C.; Schröder, J.; Becker, M.: Computational homogenization analysis in finite elasticity: material and structural instabilities on the micro– and macro–scales of periodic composites and their interaction. *Comp. Meth. Appl. Mech. Engrg.*, 191, (2002), 4971–5005.

Mielke, A.; Theil, F.: A mathematical model for rate-independent phase transformations with hysteresis. In: R. B. H.-D. Alber; R. Farwig, eds., *Proceedings of the Workshop on Models of Continuum Mechanics in Analysis and Engineering* (1999).

Mielke, A.; Theil, F.; Levitas, V.: A variational formulation of rate-independent phase transformations using an extremum principle. *Arch. Rat. Mech. Anal.*, 162 (2), (2002), 137–177.

Morrey, C. B.: Quasi–convexity and the lower semicontinuity of multiple integrals. *Pacific J. Math.*, 2, (1952), 25–53.

Onsager, L.: Reciprocal relations in irreversible processes i. *Phys. Rev.*, 37, (1931a), 405–426.

Onsager, L.: Reciprocal relations in irreversible processes ii. *Phys. Rev.*, 38, (1931b), 2265–2279.

Ortiz, M.; Repetto, E.: Nonconvex energy minimization and dislocation structures in ductile single crystals. *J. Mech. Phys. Sol.*, 47, (1999), 397–462.

Ortiz, M.; Stainier, L.: The variational formulation of viscoplastic constitutive updates. *Comp. Methods Appl. Mech. Engrg.*, 171, (1999), 419–444.

Pagano, S.; Alart, P.; Maisonneuve, O.: Solid-solid phase transition modelling. Local and global minimizations of non-convex and relaxed potentials. Isothermal case for shape memory alloys. *Int. J. Eng. Sci.*, 36, (1998), 1143–1172.

Pierard, O.; Friebel, C.; Doghri, I.: Mean-field homogenization of multi-phase thermo-elastic composites: a general framework and its validation. *Composites Science and Technology*, 64, 10-11, (2004), 1587–1603.

Pierard, O.; LLorca, J.; Segurado, J.; Doghri, I.: Micromechanics of particle-reinforced elasto-viscoplastic composites: Finite element simulations versus affine homogenization. *International Journal of Plasticity*, 23, 6, (2007), 1041–1060.

Reuss, A.: Berechnung der Fließgrenze von Mischkristallen auf Grund der Plastizitätsbedingung für Einkristalle. *Z. Angew. Math. Mech.*, 9, (1929), 49–58.

Shaw, J. A.; Kyriakides, S.: Thermomechanical aspects of NiTi. *J. Mech. Phys. Sol.*, 43, (1995), 1243–1281.

Ŝilhavy, M.: *The Mechanics and Thermodynamics of Continuous Media*. Springer (1997).

Ŝittner, P.; Liu, Y.; Novak, V.: On the origin of Lüders-like deformations of NiTi shape memory alloys. *J. Mech. Phys. Sol.*, 53, (2005), 1719–1746.

Smyshlyaev, V.; Willis, J.: On the relaxation of a three-well energy. *Proc. R. Soc. London A*, 455, (1998), 779–814.

Strutt, J. W.: Some general theorems relating to vibrations. *Proc. Lond. Math. Soc.*, 4, (1873), 357–368.

Stupkiewicz, S.; Petryk, H.: Modelling of laminated microstructures in stress-induced martensitic transformations. *J. Mech. Phys. Sol.*, 50, (2002), 2303–2331.

Tadaki, T.; Nakata, Y.; Shimizu, K.; Otsuka, K.: Crystal structure, composition and morphology of a precipitate in an aged Ti–51 at%Ni shape memory alloy. *Transactions of the Japan Institute of Metals*, 27, (1986), 731–740.

Tirry, W.; Schryvers, D.: Quantitative determination of strain fields around Ni_4Ti_3 precipitates in NiTi. *Acta Materialia*, 53, (2005), 1041–1049.

Voigt, W.: Über die Beziehung zwischen den beiden Elastizitätskonstanten isotroper Körper. *Wied. Ann.*, 38, (1889), 573–587.

Zheng, Q. S.; Du, D. X.: An explicit and universally applicable estimate for the effective properties of multiphase composites which accounts for inclusion distribution. *Journal of the Mechanics and Physics of Solids*, 49, 11, (2001), 2765–2788.

Addresses: Dr.-Ing. Thorsten Bartel, Institut für Mechanik, TU Dortmund, D-44227 Dortmund and Prof. Dr. rer. nat. Klaus Hackl, Institut für Mechanik, Ruhr-Universität Bochum, D-44780 Bochum .
email: `thorsten.bartel@udo.edu; klaus.hackl@rub.de`.